Extending Qualitative Reconstruction to Biharmonic Scattering with Limited Data

General Ozochiawaeze[1] Isaac Harris[1] Peijun Li[2]

[1] Department of Mathematics, Purdue University
[2] Chinese Academy of Sciences

SIAM Conference on Analysis of Partial Differential Equations (PD25)
November 17, 2025

Registration and travel support for this presentation was provided by the Society for Industrial and Applied Mathematics.

Paper on arXiv:

Direct & Inverse Scattering

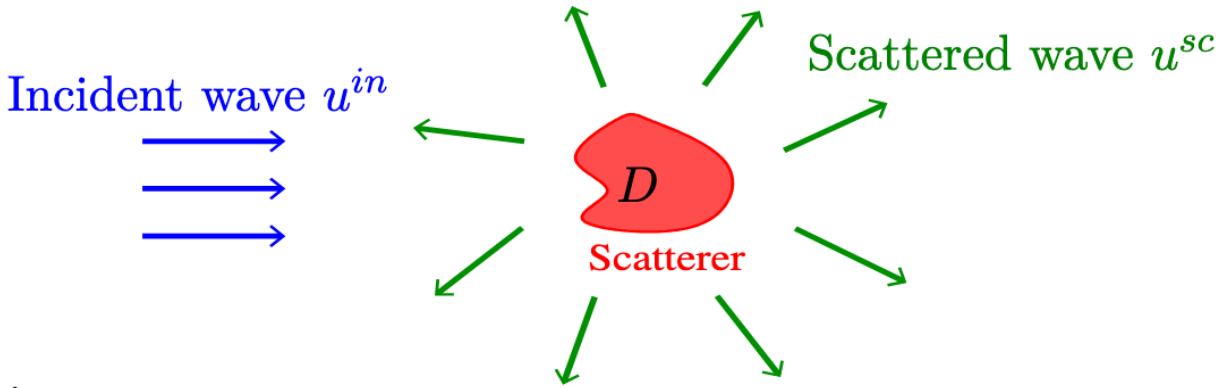

$$\begin{cases} u \text{ governed by a partial differential equation} \\ u = u^{\text{in}} + u^{\text{sc}} \quad \text{(total wave)} \\ u^{\text{sc}} \text{ is an outgoing wave} \quad \text{(radiation condition)} \end{cases}$$

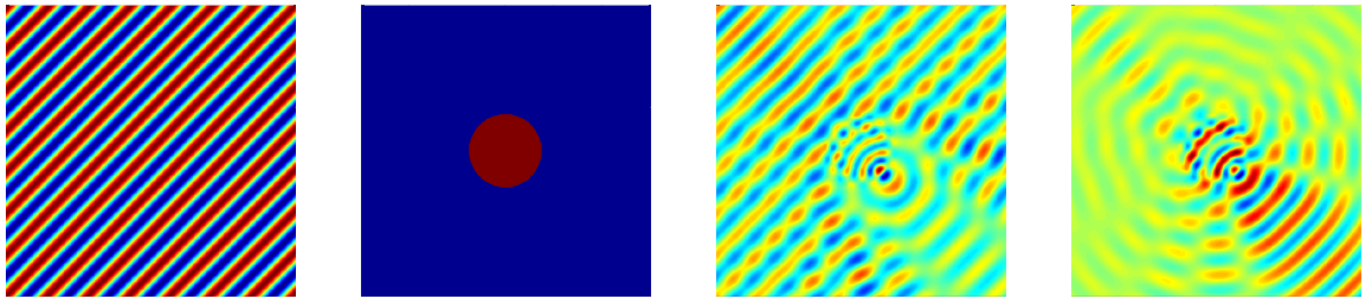

u^{in} scatterer u u^{sc}

Direct & Inverse Scattering

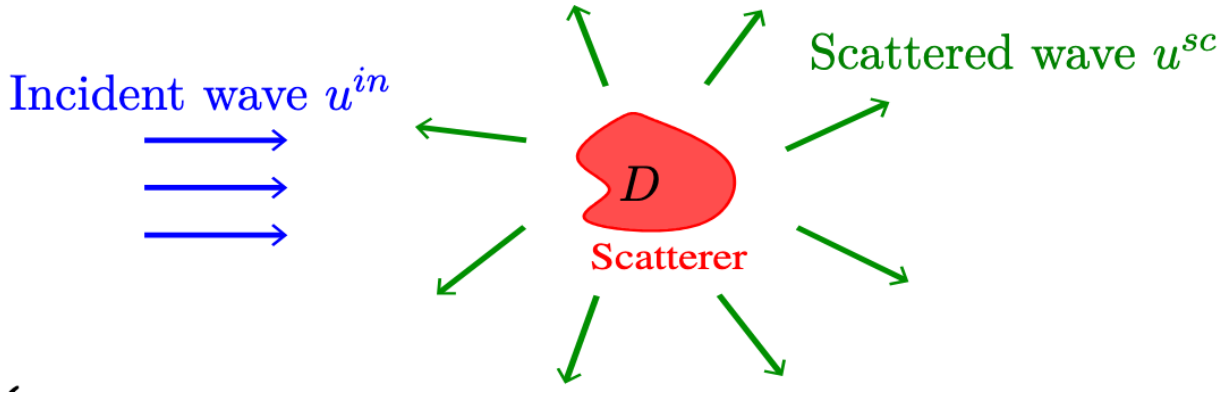

1. **Direct Problem:** Given incident wave u^{in} and scatterer D, find the scattered wave u^{sc}.
2. **Inverse Problem:** Given the far-field of scattered wave u^{sc}, find the scatterer D.

Inverse Problem (Limited Data)

Given the far-field from a **single** incident wave, determine the **location** of the scatterer D.

Setting: Wave Interaction with Thin Elastic Plates

- Out-of-plane displacement $u = u^{\text{in}} + u^{\text{sc}}$ satisfies the **biharmonic wave equation**

  $(\Delta^2 - k^4)u = 0$ in the plate (outside the cavity), $k =$ wavenumber/frequency.

- **Bilaplacian:** $\Delta^2 = \partial_{x_1}^4 + 2\partial_{x_1}^2\partial_{x_2}^2 + \partial_{x_2}^4$ (*plate bending operator*)
- A cavity (hole in the plate) perturbs the vibrated plate.
- **Goal:** Estimate the **location** of the cavity from far-field biharmonic data.

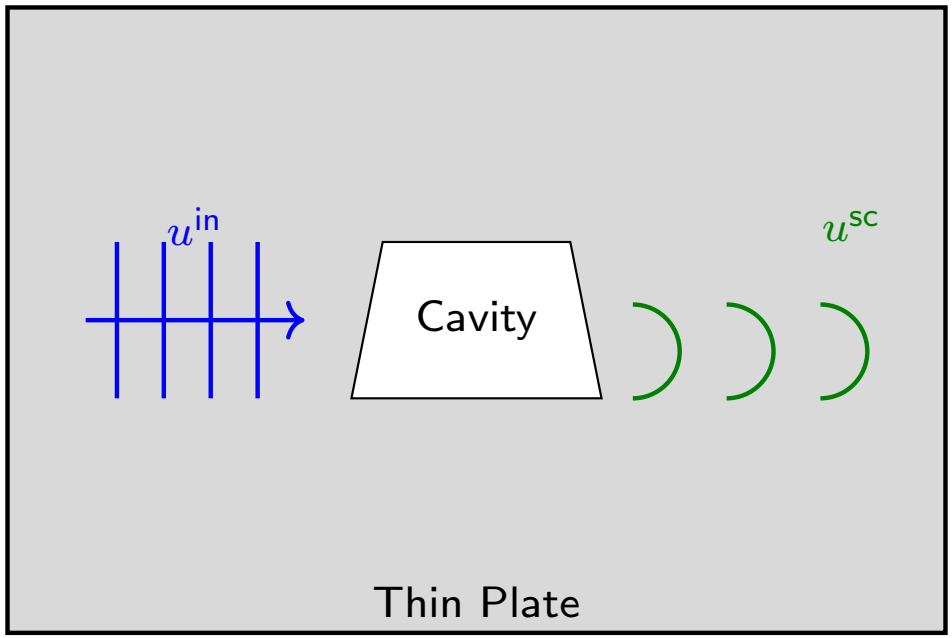

Biharmonic Clamped Scattering Problem

Problem setup: Scattering of time-harmonic flexural waves by a 2D cavity D with boundary $\Gamma = \partial D$. Find $u \in H^2_{\text{loc}}(\mathbb{R}^2)$ such that

$$\begin{cases} \Delta^2 u - \kappa^4 u = 0, & x \in \mathbb{R}^2 \setminus \overline{D}, \\ u = 0, \quad \partial_\nu u = 0, & x \in \Gamma, \ \text{(clamped boundary)}, \\ \lim\limits_{|x|\to\infty} \sqrt{|x|}\big(\partial_{|x|} u^{\text{sc}} - i\kappa u^{\text{sc}}\big) = 0, & \text{(outgoing wave)}, \\ \lim\limits_{|x|\to\infty} \sqrt{|x|}\big(\partial_{|x|} \Delta u^{\text{sc}} - i\kappa \Delta u^{\text{sc}}\big) = 0, & \text{(outgoing curvature)}. \end{cases}$$

- κ: wavenumber (frequency)
- $u = u^{\text{in}} + u^{\text{sc}}$: total displacement = incident + scattered wave
- $u^{\text{in}}(x) = e^{i\kappa x \cdot d}$, $d \in \mathbb{S}^1$ (plane incident wave)
- Clamped boundary $\Rightarrow$ both displacement and slope vanish (Dirichlet–Cauchy data)
- Far-field conditions correspond to the **Sommerfeld radiation condition (SRC)**

Well-posedness: Bourgeois–Hazard (2019), Dong–Li (2024)

Far-Field Measurements & Limited-Aperture Inverse Problem

Far-field intuition: Far from the scatterer, the scattered wave behaves like an outgoing cylindrical wave. Its amplitude and phase in each observation direction define the far-field pattern.

$$u^{\mathrm{sc}}(x) = \frac{e^{i\kappa|x|}}{\sqrt{|x|}}\, u^{\infty}(\hat{x}) + O(|x|^{-3/2}), \quad |x| \to \infty, \ \hat{x} = \frac{x}{|x|}.$$

- $u^{\infty}(\hat{x}) = u^{\infty}(\hat{x}, d_0)$: measured far-field pattern in direction $\hat{x}$ for a single incident wave d_0
- Inverse problem (single measurement): Recover the location of the scatterer D from limited far-field data $u^{\infty}(\hat{x}, d_0, \kappa)$, with fixed incident direction d_0

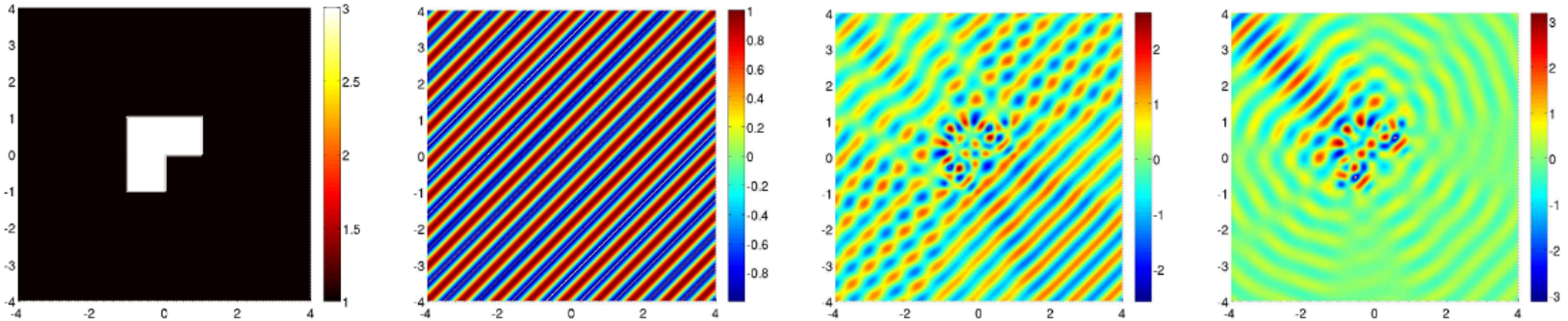

Adapted from: A. Lechleiter, *Making the Invisible Visible: Imaging Techniques for Inverse Problems* (2009)

Some Applications of Biharmonic Wave Scattering

Structural Health Monitoring
(Aircraft Industry)

Energy Harvesting
(Piezoelectric Metamaterials)

Non-Destructive Testing
(NDT / NDE)

Biharmonic ⇒ Helmholtz in the Far Field

$$(\Delta^2 - \kappa^4) = (\Delta + \kappa^2)(\Delta - \kappa^2)$$

$$u^{\text{sc}} = \underbrace{u_{\text{H}}^{\text{sc}}}_{\text{propagating}} + \underbrace{u_{\text{M}}^{\text{sc}}}_{\text{evanescent}}$$

with

$$(\Delta + \kappa^2)u_{\text{H}}^{\text{sc}} = 0, \quad (\Delta - \kappa^2)u_{\text{M}}^{s} = 0, \quad \text{in } \mathbb{R}^2 \setminus \overline{D}$$

$$\lim_{r\to\infty} \sqrt{r}(\partial_r u_{\text{H}}^{\text{sc}} - i\kappa u_{\text{H}}^{\text{sc}}) = 0, \quad \lim_{r\to\infty} \sqrt{r}(\partial_r u_{\text{M}}^{\text{sc}} - i\kappa u_{\text{M}}^{\text{sc}}) = 0.$$

Far-field behavior

Only the propagating (Helmholtz) part radiates. The evanescent part decays and does not appear at infinity.

$$\boxed{u^{\infty} = u_{\text{H}}^{\infty} \text{ (up to a constant)}}$$

Sampling Methods/Qualitative Methods

Examples of sampling methods. *Linear Sampling Method* (Colton-Kirsch, 1996), *Factorization Method* (Kirsch 1998), *Probe Method* (Potthast, 2001), *Reciprocity Gap Method* (Colton-Haddar, 2005),...)

Principle: the idea is to construct an indicator test function $\mathcal{I}(z)$ that will test whether a sampling point z is in the interior or exterior of the scatterer (i.e. $\mathcal{I}(z) \approx 1$ inside scatterer, $\mathcal{I}(z) \approx 0$ outside scatterer).

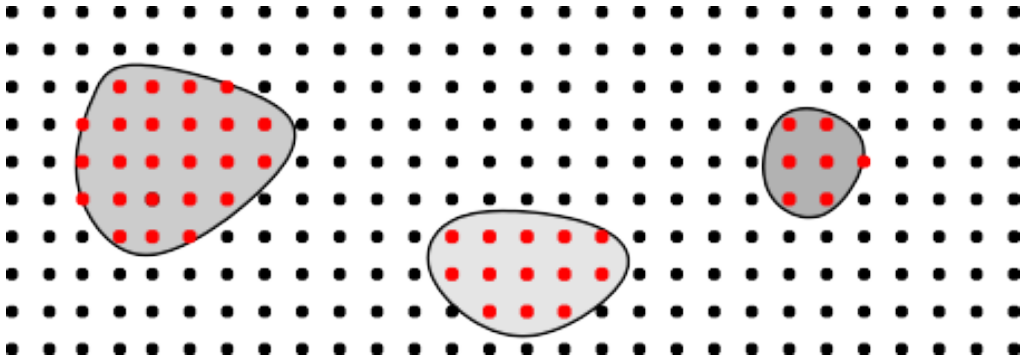

(+) Non-iterative, direct inversion, the computation of $\mathcal{I}$ does not require a forward solver.
(-) Requires a large amount of multi-static data (many transmitters-receivers).

Extended Sampling Method (ESM) Overview

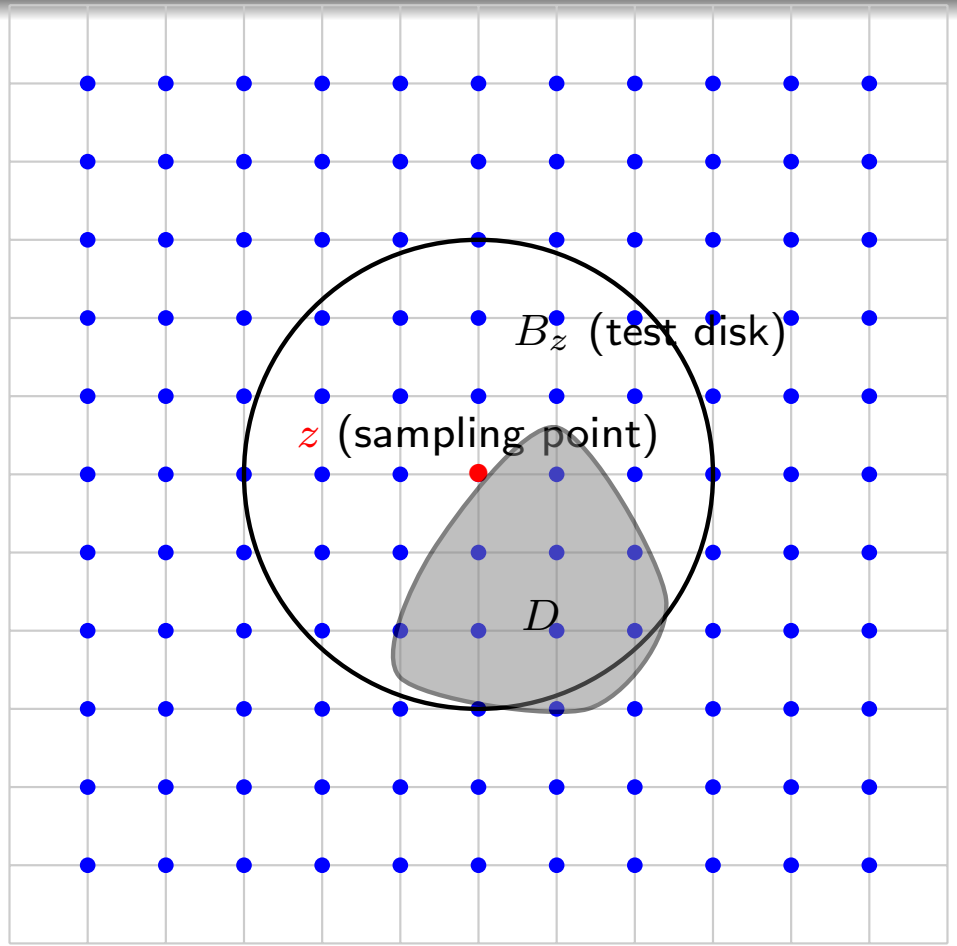

- **Key idea:** For each candidate point z, place a **template scatterer** (sound-soft disk) B_z to probe D.
- Small indicator value $\mathcal{I}(z) \Rightarrow z$ lies inside the true scatterer.
- Scanning all z yields an **indicator map** that highlights D.

Why ESM?

Why Extended Sampling?

- Versatile! Works with one-wave, multi-wave, and multifrequency data
- Effective with limited measurements
- **Our contribution:** applied to **biharmonic waves** with one or few incident wave(s) & multifrequency data

Past Applications:

- Acoustic Waves: Liu & Sun (2018), Li et al. (2020), Zeng (2020), Sun & Zhang (2023)
- Elastic Waves: Liu, J., Liu, X., & Sun (2019)

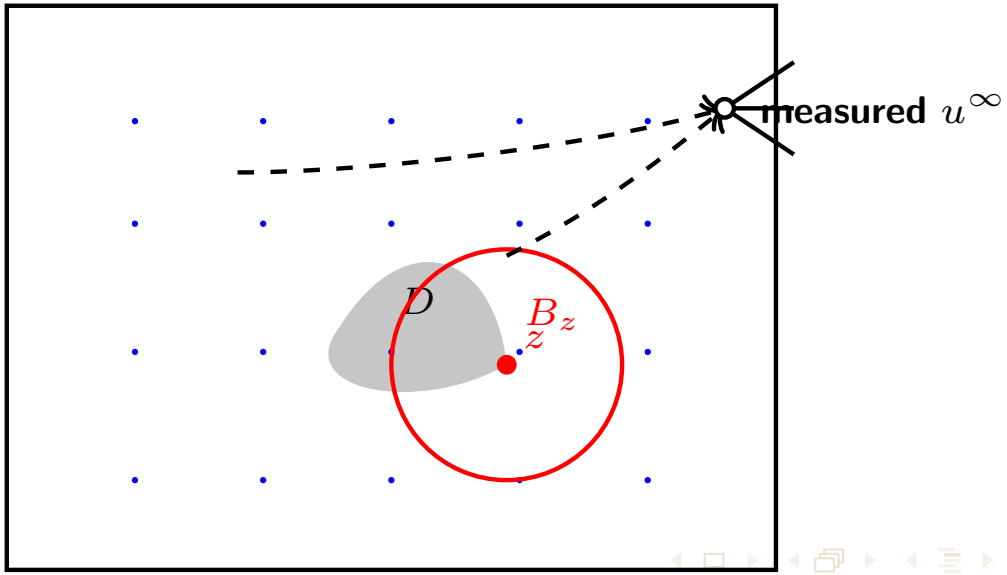

Extended Sampling Method (ESM) — Solve Far Field Equation

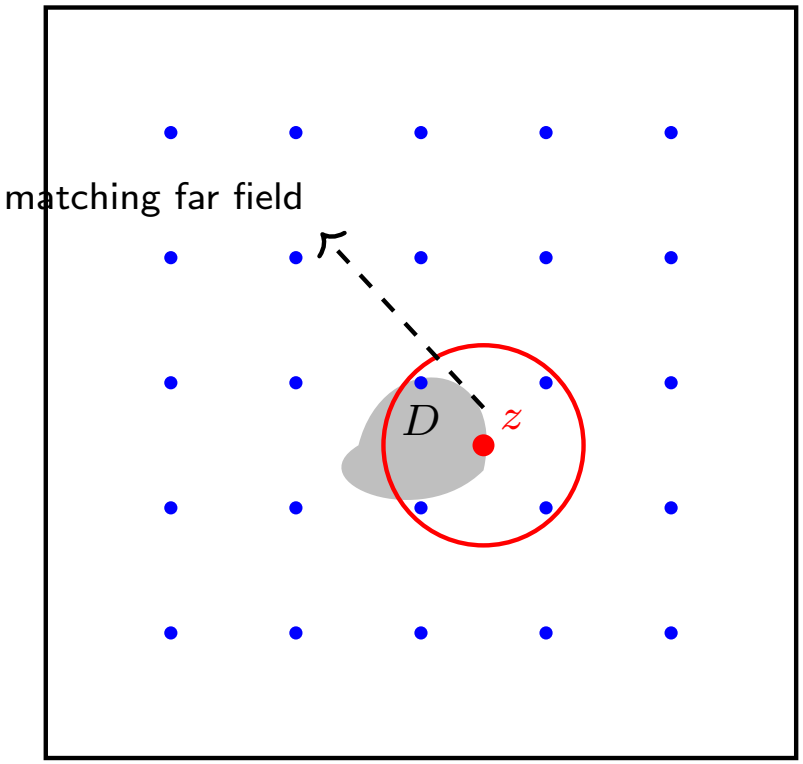

ESM Far-Field Equation

$$\mathcal{F}_{B_z} g_z \approx u^\infty(\hat{x}, d_0)$$

- $B_z = B(z, R)$ — template disk at candidate point z
- g_z — weight function over incident directions
- $\mathcal{F}_{B_z} g_z$ — weighted sum of template disk far-fields (explicit formula)
- $\mathcal{I}(z) = \|g_z\|_{L^2}$: small $\rightarrow$ z likely inside scatterer

Intuition: Scan domain; wherever weighted template far-fields match measured data, you locate the scatterer.

Ill-posed Integral Equation

The operator $\mathcal{F}_{B_z} : L^2(\mathbb{S}^1) \rightarrow L^2(\mathbb{S}^1)$ is compact with smooth kernel — hence inversion is unstable!

ESM — Rigorous Formulation

Sound-soft disk at z: Find $U^s_{B_z} \in H^1_{\text{loc}}(\mathbb{R}^2 \setminus \overline{B_z})$ such that

$$\begin{cases} \Delta U^s_{B_z} + \kappa^2 U^s_{B_z} = 0 & \text{in } \mathbb{R}^2 \setminus \overline{B_z}, \\ U^s_{B_z} + U^{\text{in}} = 0 & \text{on } \partial B_z, \\ \text{SRC at infinity}, \end{cases}$$

where $U^{\text{in}}(x, \hat{y}) = e^{i\kappa x \cdot y}$ incoming plane wave.

Far-field pattern:

$$U^\infty_{B_z}(\hat{x}, \hat{y}) = e^{i\kappa z \cdot (\hat{y} - \hat{x})}\, U^\infty_{B_0}(\hat{x}, \hat{y}), \quad U^\infty_{B_0}(\hat{x}, \hat{y}) = -\, e^{-i\pi/4} \sqrt{\tfrac{2}{\pi\kappa R}} \sum_{n=1}^{\infty} \frac{J_n(\kappa R)}{H^{(1)}_n(\kappa R)} \cos(n\theta),$$

where $\theta = \angle(\hat{x}, \hat{y})$ and $U^\infty_{B_0}$ is the closed-form far-field of a unit disk centered at the origin. **ESM operator:**

$$\mathcal{F}_{B_z} : L^2(\mathbb{S}^1) \to L^2(\mathbb{S}^1), \quad (\mathcal{F}_{B_z} g_z)(\hat{x}) = \int_{\mathbb{S}^1} g_z(\hat{y})\, U^\infty_{B_z}(\hat{x}, \hat{y})\, ds(\hat{y})$$

Indicator function: $\mathcal{I}(z) = \|g_z\|_{L^2(\mathbb{S}^1)}$ Small $\mathcal{I}(z) \to z$ likely inside scatterer.

ESM Main Idea (Theoretical Justification)

Theorem (Harris-Li-Ozochiawaeze (2025))

Let $\mathcal{F}_{B_z} : L^2(\mathbb{S}^1) \to L^2(\mathbb{S}^1)$ be the far-field operator for all test disks $B_z = B(z, R)$ for each z, and let $u^\infty(\hat{x}, d_0)$ be the measured biharmonic far field for one incident direction d_0.

Then the ESM equation

$$\mathcal{F}_{B_z} g_z \approx u^\infty(\cdot, d_0)$$

admits the following behavior:

(i) If the disk **covers the cavity** ($D \subset B_z$), there exists a stable approximate solution g_z^α with small norm.

(ii) If the disk is **disjoint from the cavity** ($D \cap B_z = \emptyset$), every such approximate solution has large norm:

$$\|g_z^\alpha\|_{L^2(\mathbb{S}^1)} \to \infty \quad \text{as } \alpha \to 0.$$

Intuition: $\mathcal{I}(z) = \|g_z^\alpha\|$ small $\Rightarrow$ z likely inside scatterer. $\mathcal{I}(z)$ large $\Rightarrow$ z outside.

Multilevel ESM: Selecting Sampling Disk Radius

Choosing the disk radius R is IMPORTANT:

- **Too large:** coarse localization, disk will capture irrelevant regions $\rightarrow$ far less precise.
- **Too small:** ESM will fail; norm may blow up unnecessarily

Multilevel strategy: start with large R to roughly capture the scatterer, then halve R iteratively for refinement.

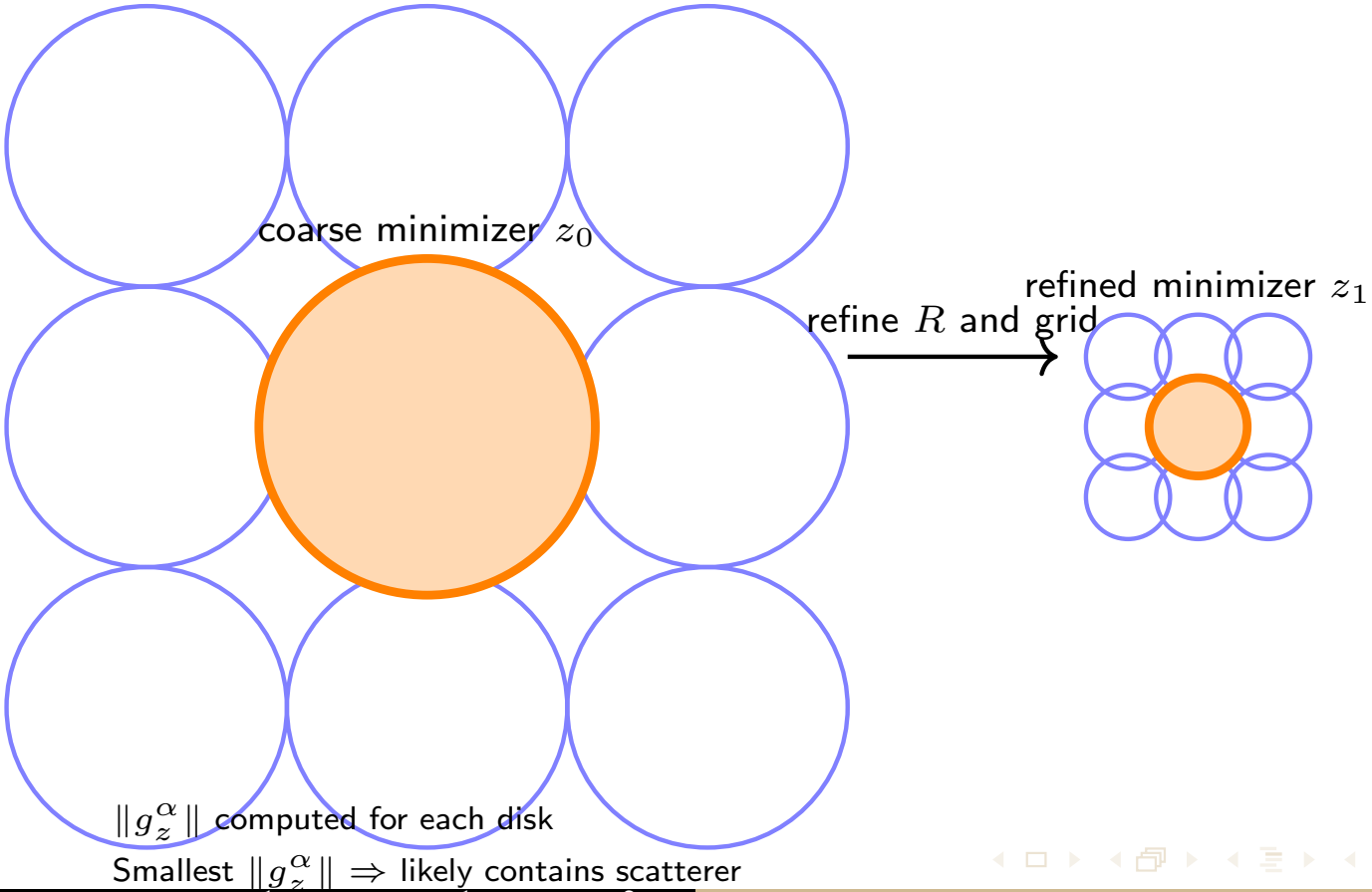

Numerical Implementation of ESM

Setup:

- Sampling grid: 200×200 equally spaced points over imaging domain.
- For each sampling point z, solve discretized ESM far-field equation using **Tikhonov regularization** with $\alpha = 10^{-4}$.

Discretized system:

$$\mathbf{A}^z \mathbf{g}_z^\alpha = u^\infty(\cdot, d_0), \quad \mathbf{A}^z_{i,j} = e^{i\kappa z \cdot (\hat{y}_j - \hat{x}_i)} U_B^\infty(\hat{x}_i, \hat{y}_j), \ i,j = 1, \ldots, 40$$

Regularized solution:

$$\mathbf{g}_z^\alpha(d) \approx ((\mathbf{A}^z)^* \mathbf{A}^z + \alpha \mathbf{I})^{-1} (\mathbf{A}^z)^* u^\infty(\cdot, d_0)$$

Discrete indicator function:

$$\mathcal{I}(z) = \frac{\|\mathbf{g}_z^\alpha\|_{\ell^2}}{\max_{z \in \mathcal{M}} \|\mathbf{g}_z^\alpha\|_{\ell^2}}$$

Cavity localization: Choose $z \in \mathcal{M}$ minimizing $\mathcal{I}(z)$ as the estimated location of the scatterer.

Multilevel ESM for Apple Cavity: Initial Localization ($R = 5$)

- Begin with a large sampling radius $R = 5$ for the disk B_z; Used $u^\infty(\hat{x}_j, d_0)$ for $j = 1, \cdots, 40$ (40 receivers) and $d_0 = (\cos \pi/3, \sin \pi/3)$ (one source), $\kappa = 2\pi$. Too Large!

$$R_0 = 5, \quad R_{j+1} = \frac{R_j}{2}.$$

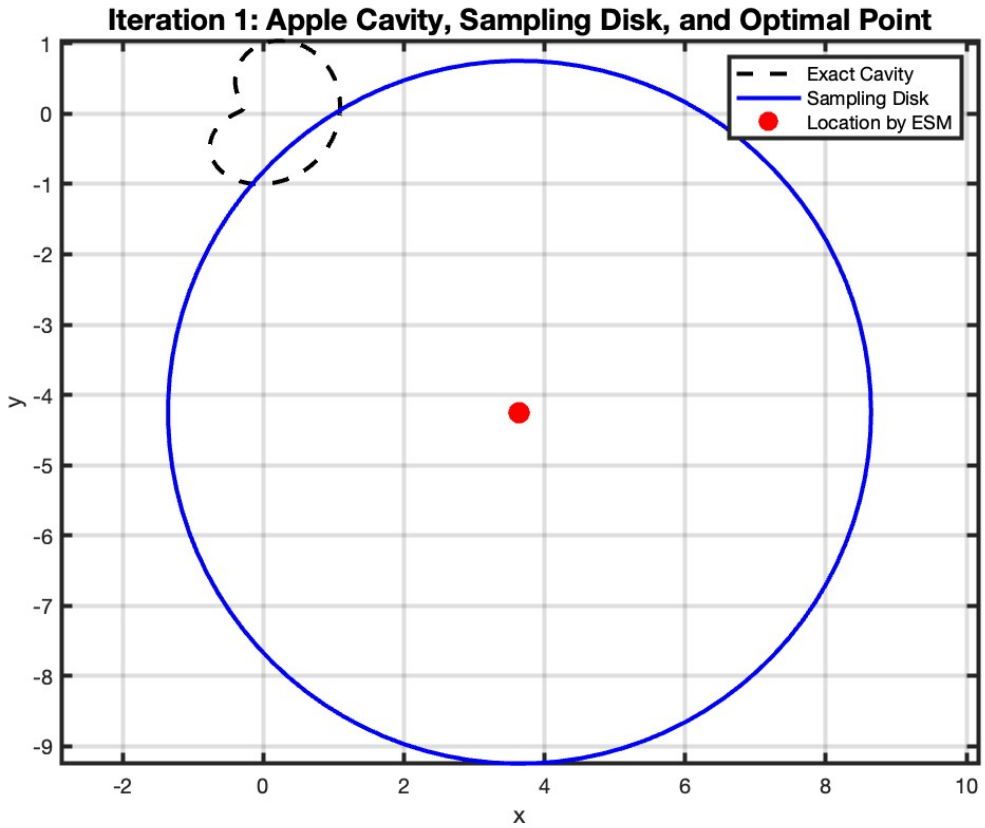

Multilevel ESM: Refinement ($R = 2.5$)

- Radius halved to $R = 2.5$. Still Too Large!

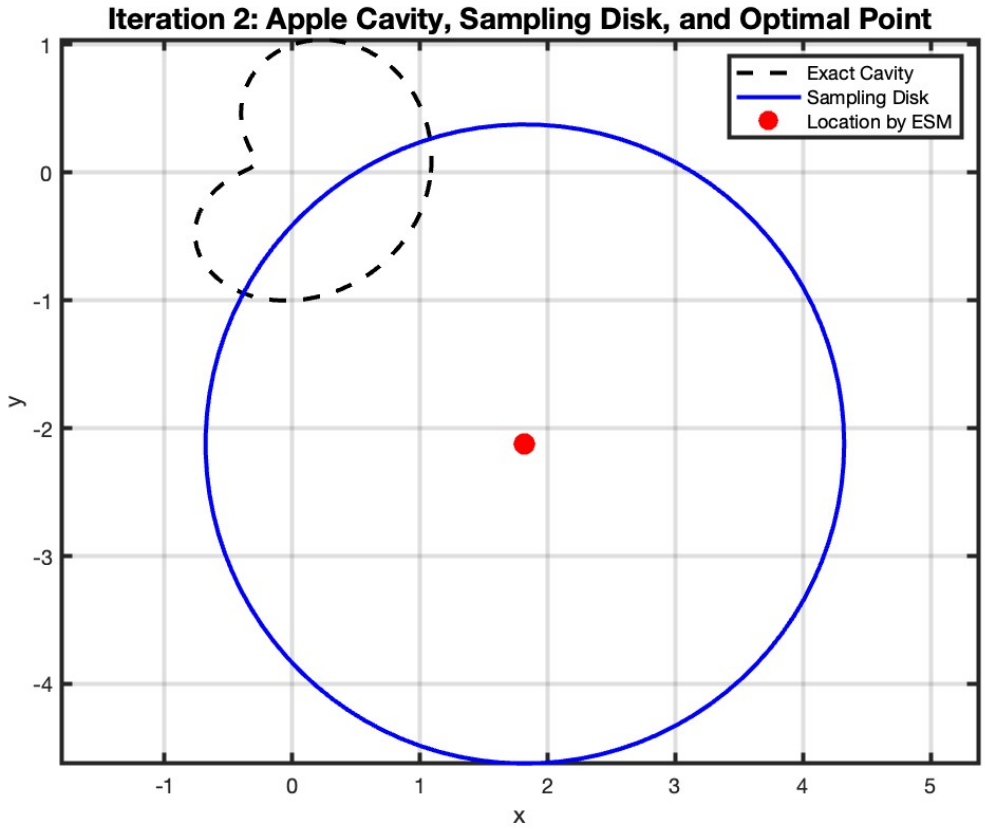

Multilevel ESM: Refinement ($R = 1.25$)

- Radius halved to $R = 1.25$. Still large!

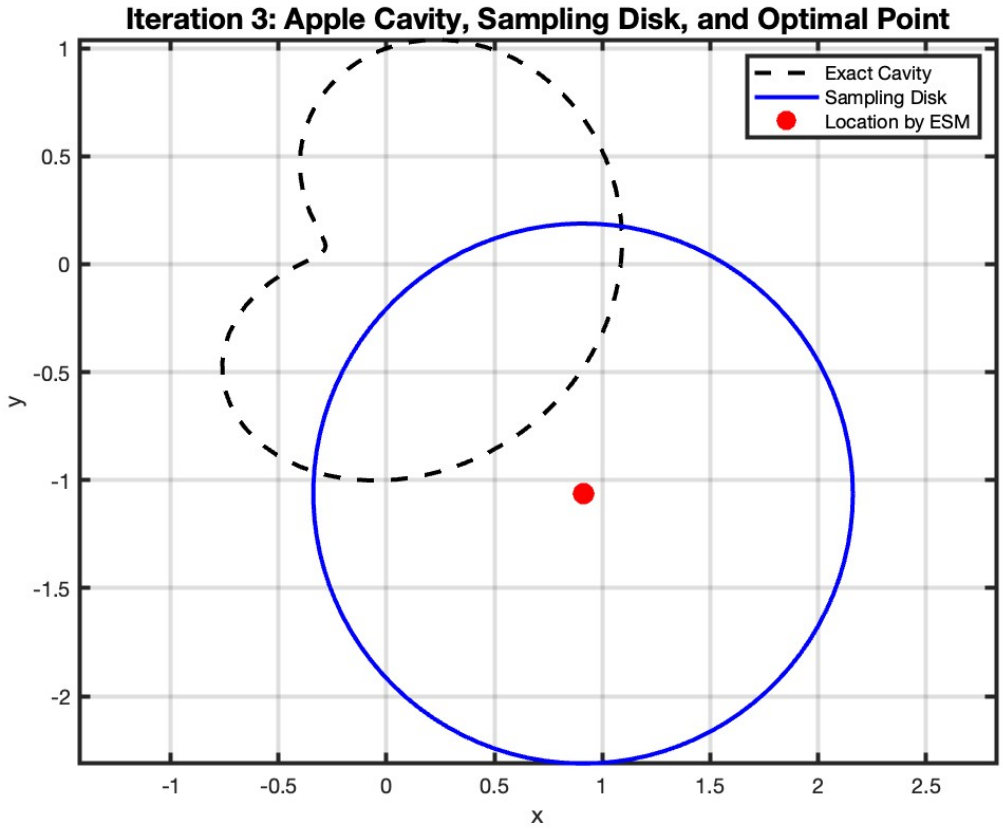

Multilevel ESM: Refinement ($R = 0.625$)

- Radius halved to $R = 0.625$, just right!

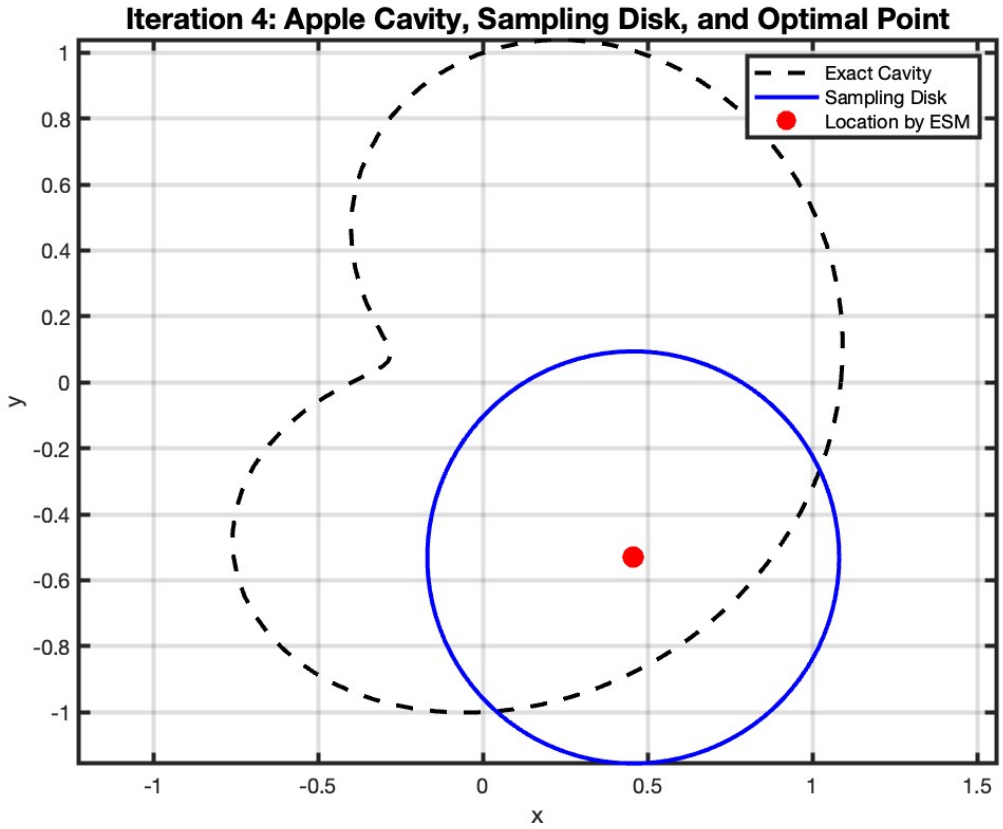

Multilevel ESM for Apple Cavity

- **Subfigures**:
  - **Apple cavity at origin** - Simulation for a cavity centered at the origin, started from initial value $R = 4$
  - **Apple cavity at (-1.5, 1.5)** - Simulation for a cavity shifted to the position (-1.5, 1.5), started from initial value $R = 5$
  - **Incident direction** $d = (1/2, \sqrt{3}/2)$ (fixed), $\kappa = 2\pi$.

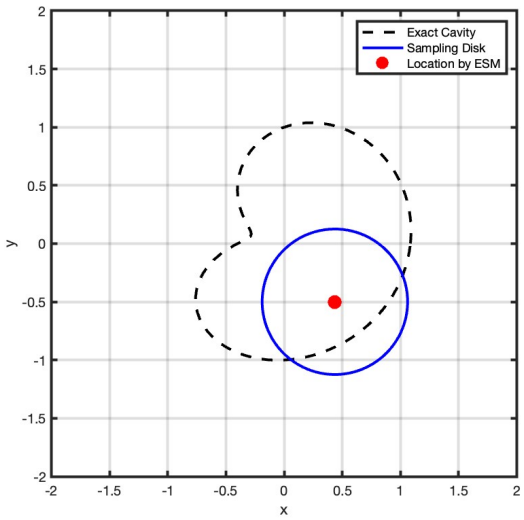

Figure: Apple cavity at origin, best radius $R = 0.5$

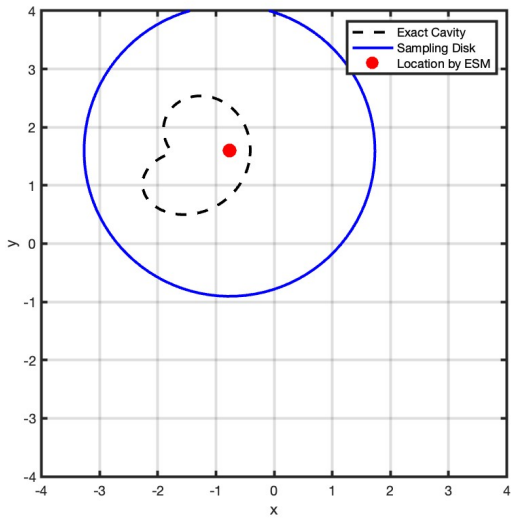

Figure: Apple cavity at (-1.5, 1.5), best radius $R = 2.5$

Multilevel ESM for Peach Cavity

- **Peach cavity at origin** - Simulation for a cavity centered at the origin, started from initial value $R = 4$
- **Peach cavity at (-1.5, 1.5)** - Simulation for a cavity shifted to the position (-1.5, 1.5), started from initial value $R = 5$
- **Subfigures**:
  - **Peach cavity at origin** - Simulation for a cavity centered at the origin.
  - **Peach cavity at (-1.5, 1.5)** - Simulation for a cavity shifted to the position (-1.5, 1.5).
  - **Incident direction** $d = (1/2, \sqrt{3}/2)$ (fixed) and $\kappa = 2\pi$.

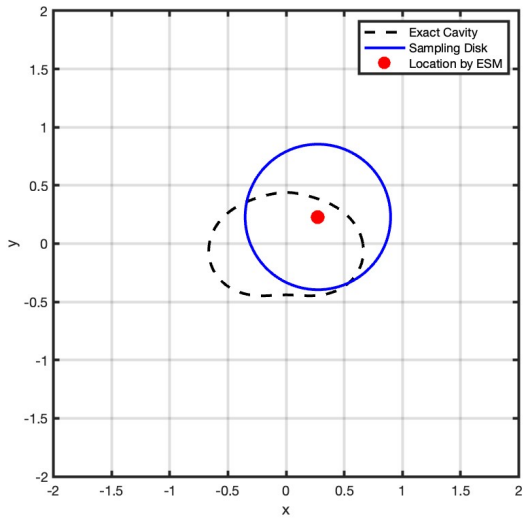

Figure: Peach cavity at origin, best radius $R = 0.5$

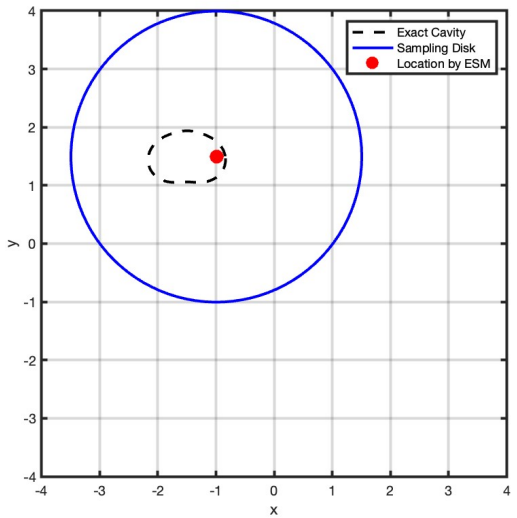

Figure: Peach cavity at (-1.5, 1.5), best radius $R = 2.5$

Indicator with Multiple Directions and Frequencies

- In practice, far-field data are measured at finitely many incident directions

$$d_j \in \mathbb{S}^1_{\text{inc}} = \{d_1, \ldots, d_J\} \subseteq \mathbb{S}^1.$$

- For each d_j, solve the regularized system

$$(\mathcal{F}_{B_z} g)(\cdot; d_j) = u^\infty(\cdot, d_j)$$

to obtain $g_z^\alpha(\cdot; d_j)$.

Multi-direction indicator:

$$\mathcal{I}(z) = \sum_{j=1}^{J} \|g_z^\alpha(\cdot; d_j)\|_{L^2(\mathbb{S}^1)}.$$

Multi-frequency extension:

$$\mathcal{I}(z) = \sum_{\ell=1}^{L} \sum_{j=1}^{J} \|g_z^\alpha(\cdot; d_j, \kappa_\ell)\|_{L^2(\mathbb{S}^1)}.$$

- Combining multiple d_j and κ_ℓ improves approximation of location from limited data at multiple fixed radii.

ESM: Multiple Incident Directions for Peach Cavity

$\mathbb{S}^1_{\mathbf{inc},1}$: $\theta = j\pi/8$, $j = 0, \ldots, 4$

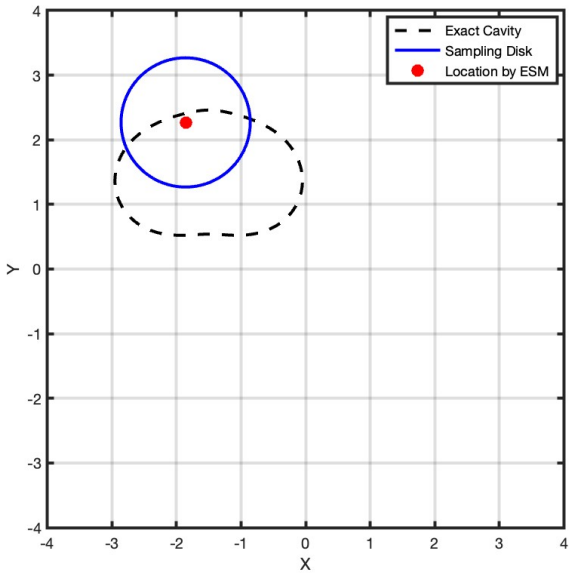

Peach cavity at $(-1.5, 1.5)$ with 5 incident directions, $R = 1$ (fixed)

$\mathbb{S}^1_{\mathbf{inc},2}$: $\theta = j\pi/5$, $j = 0, \ldots, 9$

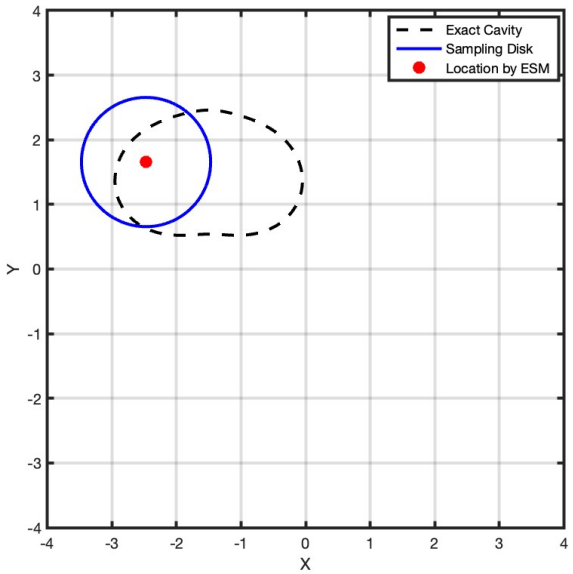

Peach cavity at $(-1.5, 1.5)$ with 10 incident directions, $R = 1$ (fixed)

ESM: Multiple Incident Directions for Peach Cavity

$\mathbb{S}^1_{\mathbf{inc},1}$: $\theta = j\pi/8$, $j = 0, \ldots, 4$

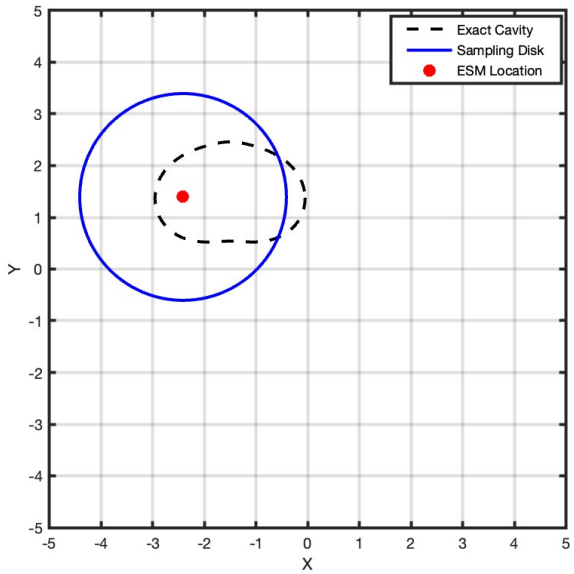

Peach cavity at $(-1.5, 1.5)$ with 5 incident directions, $R = 2$ (fixed)

$\mathbb{S}^1_{\mathbf{inc},2}$: $\theta = j\pi/8$, $j = 0, \ldots, 4$

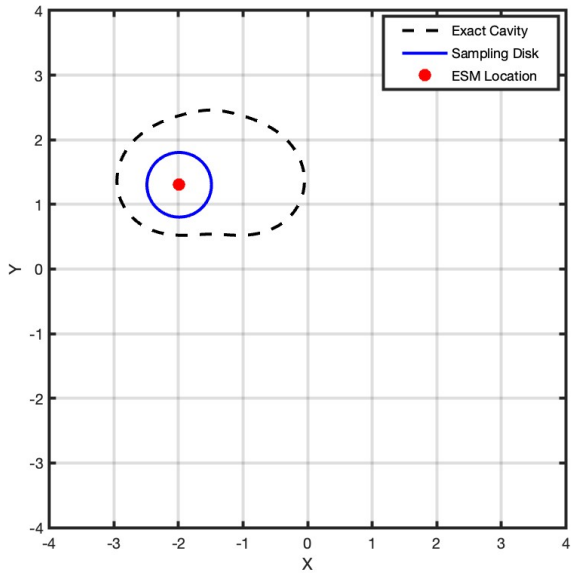

Peach cavity at $(-1.5, 1.5)$ with 5 incident directions, $R = 0.5$ (fixed)

Multifrequency ESM: Peach Cavity at $(-1.5, 1.5)$

- **Objective**: Simulate scattering from a peach-shaped cavity across multiple frequencies. Benefit: no need to find best radius R!
- **Frequency Range**:

$$[\kappa_{\min}, \kappa_{\max}] = \begin{cases} [\pi, 2\pi] & \text{(first frequency range)} \\ [\frac{\pi}{3}, 5\pi] & \text{(second frequency range)} \end{cases}$$

- **Input Data**:
  - $u^{\infty}(\hat{x_i}, d, \kappa_\ell)$: Far-field data for various incident directions and frequencies.
  - Incident direction $d = (1/2, \sqrt{3}/2)$ (fixed). Radius $R = 1$ (fixed)
  - Frequencies: κ_ℓ chosen at 5 distinct frequencies within the specified range.

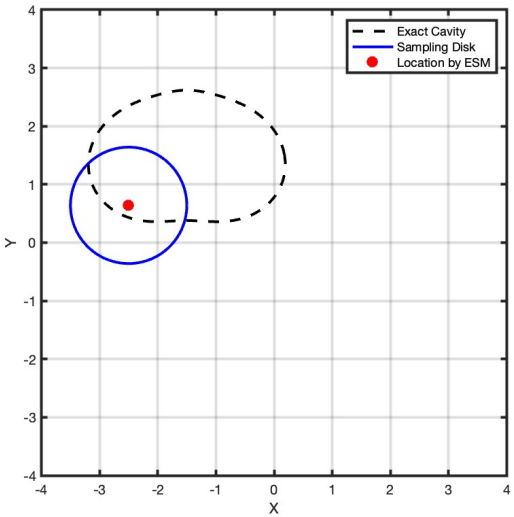

Figure: Peach cavity with range $[\pi, 2\pi]$

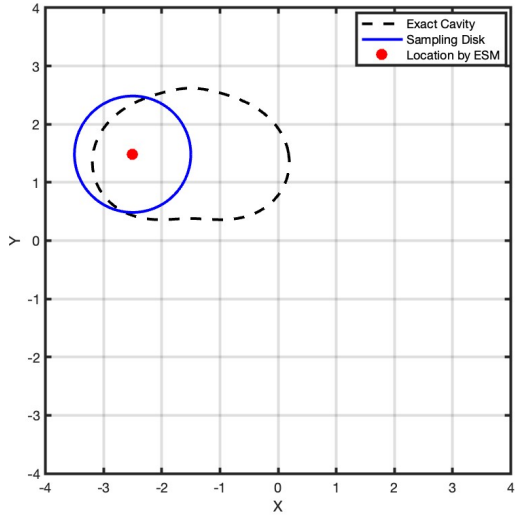

Figure: Peach cavity with range $[\frac{\pi}{3}, 5\pi]$

Conclusion & Outlook

- **ESM successfully localized a cavity scatterer** in the biharmonic setting with limited data.
- **Future work:** use as initial guess for iterative or Bayesian schemes, explore hybrid methods, and test different boundary conditions.

References:

- H. Dong and P. Li, *A novel boundary integral formulation for the biharmonic wave scattering problem*, J. Sci. Comput., 98 (2024), 42:1–29.
- H. Dong and P. Li, *Uniqueness of an inverse cavity scattering problem for the biharmonic wave equation*, Inverse Problems, 40 (2024), 065011.
- I. Harris, P. Li, and G. Ozochiawaeze, *Sampling methods for the inverse cavity scattering problem of biharmonic waves*, arXiv preprint (2025).
- J. Liu and J. Sun, *Extended sampling method in inverse scattering*, Inverse Problems, 34 (2018), 085007.
- Z. Li, Z. Deng, and J. Sun, *Extended-Sampling-Bayesian Method for Limited Aperture Inverse Scattering Problems*, SIAM J. Imaging Sci., 13 (2020).